Journal of Environmental Biology
p-ISSN: 0254-8704 • e-ISSN: 2394-0379 • CODEN: JEBIDP

JEB®

Original Research Paper
Volume 45 Issue 3 May 2024 pp. 243-252
DOI: http://doi.org/10.22438/jeb/45/3/MRN-5218

J. Environ. Biol., 2024

Journal website : www.jeb.co.in ★ E-mail : editor@jeb.co.in

Antimicrobial and anti-inflammatory efficiency of green synthesized zinc oxide nanoparticles using *Polianthes tuberosa* flower concentrate

J.J.A. Christy[1], S.B. Begum[2], M. Revathy[1], B.R Harisma[1] and R.M. Murugappan[1]*

[1]*Department of Zoology, Thiagarajar College, Madurai-625 009, India*
[2]*PG and Research Department of Zoology, V.O. Chidambaram College, Tuticorin-628 008, India*

Received: 04 January 2024 **Revised:** 05 March 2024 **Accepted:** 08 April 2024

***Corresponding Author Email :** murugu19@gmail.com ***ORCiD:** https://orcid.org/0009-0006-9479-8966

Abstract

Aim: In the present study, zinc oxide nanoparticles (ZnO NPs) were synthesized using *Polianthes tuberosa* flower concentrate. Antimicrobial and anti-inflammatory efficiency of the green synthesized ZnO NPs were analysed under *in vitro* conditions.

Methodology: Nanoparticles formation was confirmed by UV-visible spectroscopy. Size, shape and morphology of the green synthesized ZnO NPs was determined by SEM coupled with EDAX and AFM. Molecular and elemental compositions of the nanoparticle were determined by XRD and FT-IR analyses.

Results: X-ray diffraction analysis depicted the hexagonal wurtzite structure of ZnO NPs with a particle size of 80 nm. The FT-IR analysis illustrated the functional groups responsible for the encapsulation and stabilization of ZnO NPs. At micromolar concentration, ZnO NPs was found to inhibit the growth of selected skin pathogens and suppress biofilm formation in *Pseudomonas aeruginosa.*

Interpretation: *P. tuberosa* flower concentrate and green synthesized ZnO Nps inhibited the growth of bacterial and fungal pathogen in a dose-dependent manner. Biofilm inhibitory efficiency and anti-inflammatory activity of the zinc oxide nanoparticle illustrated that it can be used for treating skin infections.

Key words: Anti-biofilm, Anti-inflammatory, *Polianthes tuberosa*, Zinc oxide nanoparticles

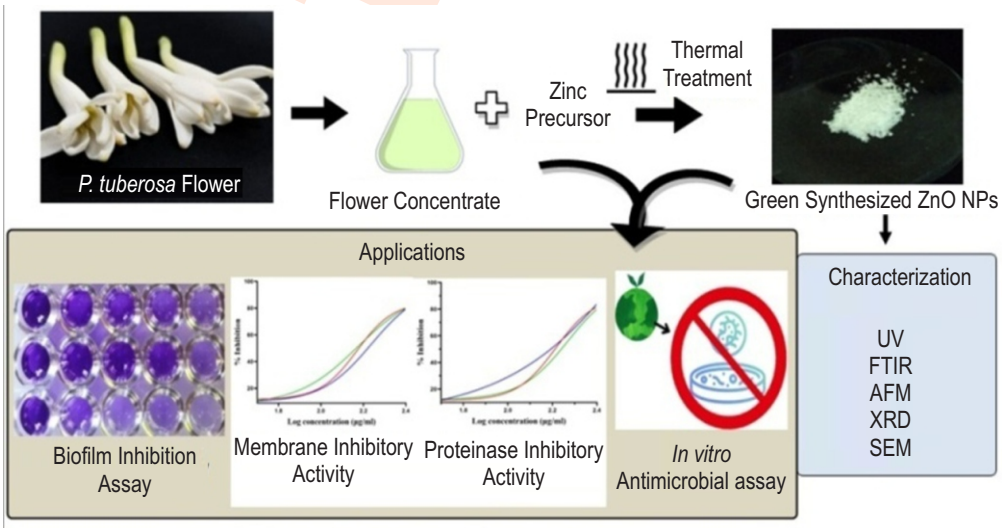

How to cite: Christy, J.J.A., S.B. Begum, M. Revathy, B.R Harisma and R.M. Murugappan: Antimicrobial and anti-inflammatory efficiency of green synthesized zinc oxide nanoparticles using *Polianthes tuberosa* flower concentrate. *J. Environ. Biol.*, **45,** 243-252 (2024).

Introduction

Plants and plant-based products have been used as a source of drug constituent in modern medicine. Since antiquity, phytochemicals are used in the treatment of inflammations and infections induced by insects and microbes (Alves *et al.,* 2020). The burgeoning worldwide interest in herbal remedies reflects the recognition of traditional claims in health care. Medicinal herbs being natural are safe and considered as a viable alternative to synthetic drugs (Agidew, 2022). Tuberose (*Polianthes tuberosa* L.), an economically important perennial floriferous herb of family Agavaceae (formally known as Amaryllidaceae) is cultivated worldwide for its fragrant, waxy, star-shaped white florets. *P. tuberosa* flower oil is used extensively in cosmetics and perfume industry (Qureshi *et al.,* 2018). Apart from its applications in personal skin care products, the plant is bestowed with medicinal properties (Alghuthaymi *et al.,* 2023). However, only a handful of reports are available in support of the medicinal value of *P. tuberosa* (Suryakoppa *et al.,* 2021). The bulbs and flowers of *P. tuberosa* abounds with benzenoids, phenyl propanoids, terpenoids, nitrogen, sulphur containing compounds and few fatty acid derivatives (McIntosh *et al.,* 2018).

The phytochemical constituents in the flowers of *P. tuberosa* possess antimicrobial, cytotoxic, membrane stabilizing and thrombolytic activities (Kutty and Mitra, 2019). The pristine substrates in the flowers of *P. tuberos*a are rich in amino, carboxyl and hydroxyl groups which are commonly used as a stabilizing and capping agents in the biosynthesis of metal nanoparticles (Sidhu *et al.,* 2022). The above rationale directed to use the flower of *P. tuberosa* in medicinal nanoscience to mitigate myriad health maladies. Topical application of commercially available synthetic ointments is reported to cause skin allergies and dysbiosis of the microflora. To evade the imbalance, certain bacteria form biofilms (Wang *et al.,* 2017). Biofilm forming bacteria are resilient to immune system, UV-light, antibiotics, chemicals, disinfectants, etc. (Vestby *et al.,* 2020). Therefore, there is an everlasting demand for plant based skin care products. The essential oil extracted from the flowers of *P. tuberosa* were used in the treatment of skin rashes and bacterial skin infections (Setiani *et al.,* 2020).

Application of plant-based skin care products has certain limitations of poor solubility, less stability, low permeability and active efflux process. The above hindrances can be overcome by reducing the particle size of the therapeutically efficient plant-based products to nanoscale. Downsizing the chemicals induces systemic activity due to greater mobility of particles (Patravale *et al.,* 2004). Biofabrication of metal nanoparticles using medicinal plants is in limelight because of their enhanced physiological and biological properties (Sepasgozar *et al.,* 2021). The green synthesis approach is advantageous over conventional methods because of its low cost, high stability, biological safety, with greater catalytic activity and large-scale biosynthesis of nanoparticles with zero environmental toxicity (Alhujaily *et al.,* 2022). Of the different metals, utilization of zinc oxide has piqued the curiosity due to its biocompatible, less toxic nature and versatile biological activity. ZnO is one of the ingredients used in creams, lotions and ointments due to its antibacterial activity (Raha and Ahmaruzzaman, 2022). ZnO is considered to be a "GRAS" (generally recognized as safe) substance by the FDA. The intrinsic properties of zinc oxide, also known as Zincite make it an excellent candidate as the material of choice for nanoparticle synthesis. Multiplicity of process is involved in zinc oxide nanoparticles (ZnO NPs) synthesis. However, the process adopted for fabrication influence the properties, thereby indirectly influence its stability and suitability for various applications. The antibacterial efficiency of green synthesized ZnO NPs using the leaves of *Cassia fistula* and *Melia azadarach* was reported by Naseer *et al.* (2020). El-Belely *et al.* (2021) evaluated the antimicrobial and cytotoxic effect of ZnO NPs biofabricated using the microalaga *Arthrospira platensis.* Nazir *et al.* (2022) demonstrated the photocatalytic and antibacterial potential biofabricated ZnO NPs. elucidated that Zinc-based nanoparticles inhibit formation of bacteria mediated biofilm. Recently, Fulindi *et al.* (2023).

Therefore, in this study, an attempt was made to synthesise ZnO NPs using flowers of *P. tuberosa* rather than the leaves. In order to determine the size, structure, elemental composition, functional groups present and physical properties, the green synthesized ZnO NPs was subjected to UV-Vis spectrophotometer, FT-IR, SEM coupled with EDAX, AFM and XRD analyses. Furthermore, the therapeutic potential of the green synthesized ZnO NPs was determined by biofilm inhibition, anti-inflammatory and antimicrobial activity.

Materials and Methods

Analyses of phytochemical constituents: Fresh *Polianthes tuberosa* flowers were collected washed, shade dried and powdered. The flower powder (10 gm) was boiled at 45°C for 30 min with 10ml of milli-Q water. The resultant solution was filtered using Whatman No.1 filter paper and concentrated at 45° C under reduced pressure in a rotary evaporator (Manjamalai *et al*., 2010). The phytochemical phenolic and flavonoid constituents in the flower concentrate were analysed following the method (Harborne, 1973; Sofowara, 1993).

Synthesis of zinc oxide nanoparticles: The flower concentrate was mixed with equal volume of 0.05 mM zinc nitrate (Sigma-Aldrich Chemicals, India) solution and stirred continuously at 30°C for 40 min. The mixture was cooled and incubated at 37°C for the precipitate to settle. Reduction of zinc nitrite to zinc oxide nanoparticles was confirmed with the formation of white precipitate. The precipitate was rinsed with milli-Q water and ethanol at 5000 rpm for 15 min. The purified white precipitate (ZnO NPs) was dried for 7–8 hr at 80°C (Sangeetha, 2011).

Characterization of the synthesized ZnO NPs: The green synthesized ZnO NPs were subjected to UV, FT-IR, AFM, XRD, SEM and EDAX techniques to determine the size, shape, crystallographic nature, functional groups present and elemental

composition. The surface plasmon resonance peak of the flower concentrate, zinc nitrate and ZnO NPs were determined using UV–Vis double beam bio spectrophotometer (Jasco- UV-660). λ_{max} was determined by recording the spectra between 200 to 800 nm. An elemental composition of nanoparticles was examined through energy dispersive spectroscopy (EDS) using JEOL-JSM-IT200 by instrument attached to scanning electron microscopy (SEM). Phase purity, crystal nature and grain size of nanoparticles were characterized by subjecting it to powder X-ray diffractometer with Cu (Kα) radiation (ʎ = 0.1546 nm) in a transmission mode at 40 kv 30 mA with 2θ ranging from 10-90°. All experiments were carried out in triplicates and the data were analyzed using Origin Pro 7.5 SRO software (Orgin Lab Corporation, USA). The topological analyses of the nanoparticles were performed using Atomic Force Microscope Agilent-5500. The flower concentrate and the biosynthesized nanoparticles were subjected to FT-IR spectroscopy (Jasco 4600) for determination of functional groups. The spectrum ranging from 4000 to 400 cm^{-1} was recorded. The IR spectrum of the sample was an average of 45 data scanning over the entire range of wave numbers, with the resolution of 4 cm^{-1} (Chaudhuri and Malodia, 2017).

Antimicrobial activity: *In vitro* antagonistic activity of the flower concentrate and ZnO NPs towards the selected bacteria [*Micrococcus luteus* (MTCC1538), *Staphyloccocus aureus* (MTCC 2940) and *Escherichia coli* (MTCC 739)] and the fungi [*Aspergillus flavus* (MTCC 2798), *Penicillium oxalicum* (MTCC 4931), and *Fusarium oxysporum* (MTCC4894)] was determined following well diffusion method. Method described by Smania *et al.* (1999) was followed to determine the antibacterial activity with slight modifications. A 100 µl of bacterial culture at its mid log phase was spread over Muller Hinton agar plates and incubated at room temperature for a brief period of 4 hrs to promote the initial growth. To elucidate the antifungal activity method described by Gao *et al.* (2014) was followed with modifications. Fungal spore suspension (6×10^6 ml^{-1}) was mixed with Potato Dextrose Agar and transferred to the sterile petriplates. Wells were created on the agar medium with 6 mm sterile cork borer. Twenty micro litre of the flower concentrate and ZnO NPs at various concentrations (20, 40, 60, 80 and 100 µl ml^{-1}) were loaded onto the wells. A control was maintained by adding 20 µl of sterile Milli-Q water. The antibacterial and antifungal potential of flower concentrate and ZnO NPs was determined by measuring the zone of inhibition after incubation at 37°C for 24 and 48 hr respectively. Triplicates were maintained for all the experiments.

Biofilm Inhibition Assay: Biofilm inhibitory potential of ZnO NPs was determined by crystal violet (CV) assay (O'Toole *et al.,* 1999) using 96- well microtiter plate. Briefly, 180 µl of *Pseudomonas aeruginosa* (MTCC 741) suspension (10^6 CFU ml^{-1}) was transferred to the wells of the titre plate under aseptic conditions and 10 µl of ZnO NPs was loaded into the wells and incubated at 37°C for 24 hr. The unbound bacteria were removed from the wells by rinsing it with phosphate- buffered saline (pH=7.4). The cells attached to the surface were fixed with 70% ethanol and stained with 100 µl 0.1% crystal violet up to15 min at 37°C. The excess stain was discarded and washed with PBS. Finally, the wells were destained with 95% methanol and after 30 min the absorbance was read at 590 nm using ELISA microplate reader. The untreated wells served as a control. Sodium hypochlorite (100%) with *P. aeruginosa* served as a positive control. The percentage of biofilm inhibition was calculated along the formula:

Bio film inhibition (%) = (OD control - OD treatment)/ OD control X 100

Anti-inflammatory activity: Anti-inflammatory efficiency of *P. tuberosa* flower concentrate and biosynthesized ZnO NPs was determined under *in-vitro* conditions by membrane stabilization assay and proteinase inhibitory test. Membrane stabilization potential was determined following the procedure described by Sadique *et al.* (1989). Human blood (10 ml) was collected, pelletized (3000 rpm 10 min) and diluted to 10% with saline. Various concentrations (50, 100, 150, 200 and 250 µg ml^{-1}) of *P. tuberosa* flower concentrate and biosynthesized nanoparticle were mixed with equal volume of RBC suspension and incubated at 50°C for 30 min. The reaction mixture was centrifuged for 10 min at 3000 rpm, the optical density of the supernatant was recorded at 560 nm. In addition to a control group, Aceclofenac® the commercially available drug recommended for anti-inflammatory activity was also analysed. Proteinase inhibitory activity was determined following the procedure of Anantha (1956). The reaction mixture (2 ml) containing one ml of flower concentrate or ZnO NPs at various concentrations of 50, 100, 150, 200, 250 µg ml^{-1}, 0.06 mg trypsin, 1 ml of 20 mM tris-HCl buffer (pH 7.4) was incubated at 37°C for 5 min. To the reaction mixture, 1ml of 0.9 % (w/v) casein was added and incubated for 25 min. The reaction was terminated adding 2 ml of perchloric acid. The resultant hazy suspension after centrifugation was read at 210 nm using buffer as a blank. Proteinase and membrane stabilization inhibitory efficiency of *P. tuberosa* flower concentrate and green synthesized ZnO NPs was subjected to dose-response statistical analysis using prism software (ver. 6.04).

Results and Discussion

Phytochemical investigations revealed the presence of tannins, saponins, flavonoids, alkaloids and terpenoids in the flowers of *P. tuberosa* except steroids (results not shown). The phenolic and flavonoid content in *Polianthes tuberosa* was determined quantitatively. It was found to be 2.15 mg ml^{-1} gallic acid equivalent and 1.35 mg ml^{-1} quercetin equivalent respectively. The aforementioned phytochemical constituents in the flowers may be responsible for the stabilization and reduction of metal ions during the green synthesis of NPs. With the support of the available literature, it was confirmed that the ZnO NPs synthesis was facilitated by the bioactive metabolites and functional groups present in the flowers of *P. tuberosa* (Yang *et al.,* 2019). Kumar *et al.* (2020) reaffirmed that the bioactive molecules such as flavonoids, terepenoids, coumarins, xanthones etc., acted as reducing and stabilizing agent in the process of flower

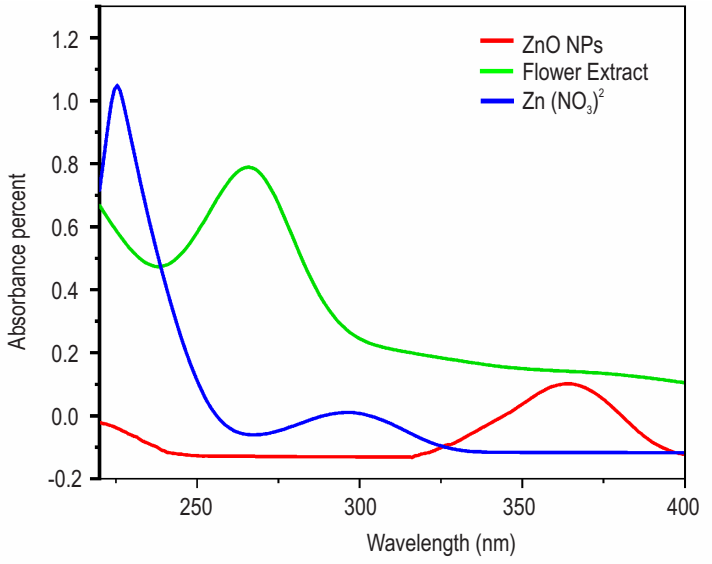

Fig. 1: UV-Vis absorption spectra of *Polianthes tuberosa* flower concentrate, ZnO NPs and Zn $(NO_3)^2$.

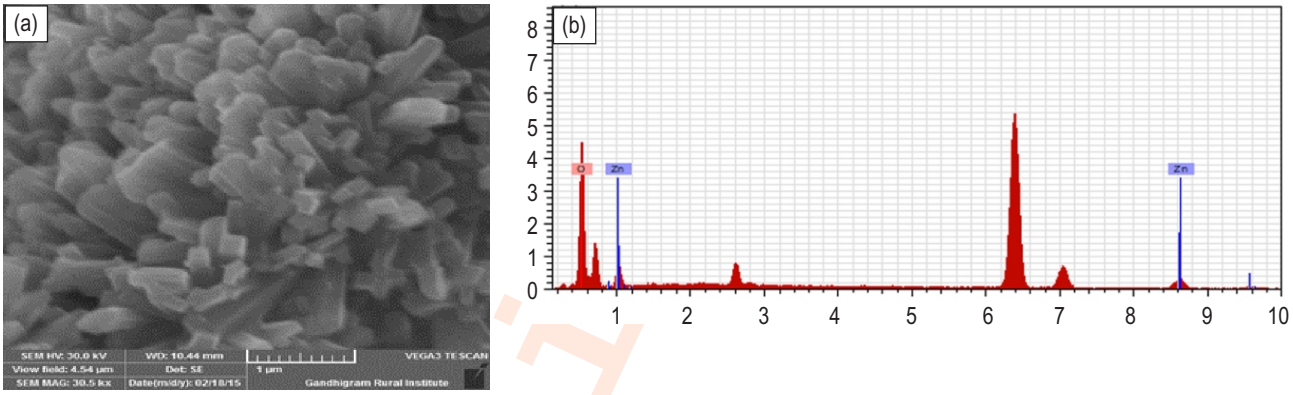

Fig. 2: Scanning electron microscopic image (a) and EDAX spectrum (b) of ZnO nanoparticles.

based green synthesis of metal Nps. UV-Visible absorption spectra of *P. tuberosa* flower concentrate, zinc nitrate, and green synthesized ZnO NPs are presented in Fig. 1. ZnO NPs exhibit an absorption peak range of 350 to 370 nm and attains an intrinsic band-gap peak at 360 nm. Broadening of the peak illustrate the agglomeration of nanoparticles. The shift to a longer wavelength by zinc nitrate solution may be due to large particle size. An absorption peak at 260 nm was observed for *P. tuberosa* flower concentrate. The reduction of $Zn(NO_3)^2$ to ZnO NPs may be due to the electron donating ability of the phenolic compounds present in the flower concentrate. The results obtained in this study satisfy the standard ZnO absorption pattern. Nithya Deva Krupa and Raghavan (2014) reported that nanoscale materials have shorter wavelengths. This notion supports the results of the present study. Krol *et al.* (2017) reported that the H-bond and electrostatic force of interaction between bioorganic capping molecules of the flower concentrate and NPs results in agglomeration. Salam *et al.* (2014) reported that when the green synthesis of nanoparticles was carried out in aqueous medium agglomeration occured.

Scanning electron microscopic imaging of ZnO NPs reaffirms the hexagonal crystal nature and agglomeration of ZnO NPs with the particle size of approximately 80 nm (Fig. 2a). The reduced particle size of green synthesized ZnO nanoparticle facilitate the water soluble nature, rapid cell membrane permeation, long retention time at the site of infection. Owing to high surface area-to-volume ratio, not only the quantity of nanoparticles needed for the biological reaction get minimized, but also the efficiency was found to be enhanced significantly. EDAX spectrum represents the elemental composition and purity

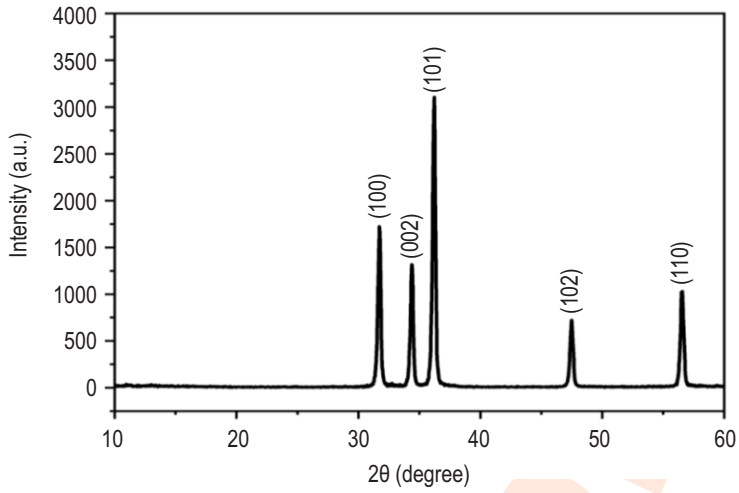

Fig. 3: X-ray diffraction pattern of green synthesized ZnO nanoparticles.

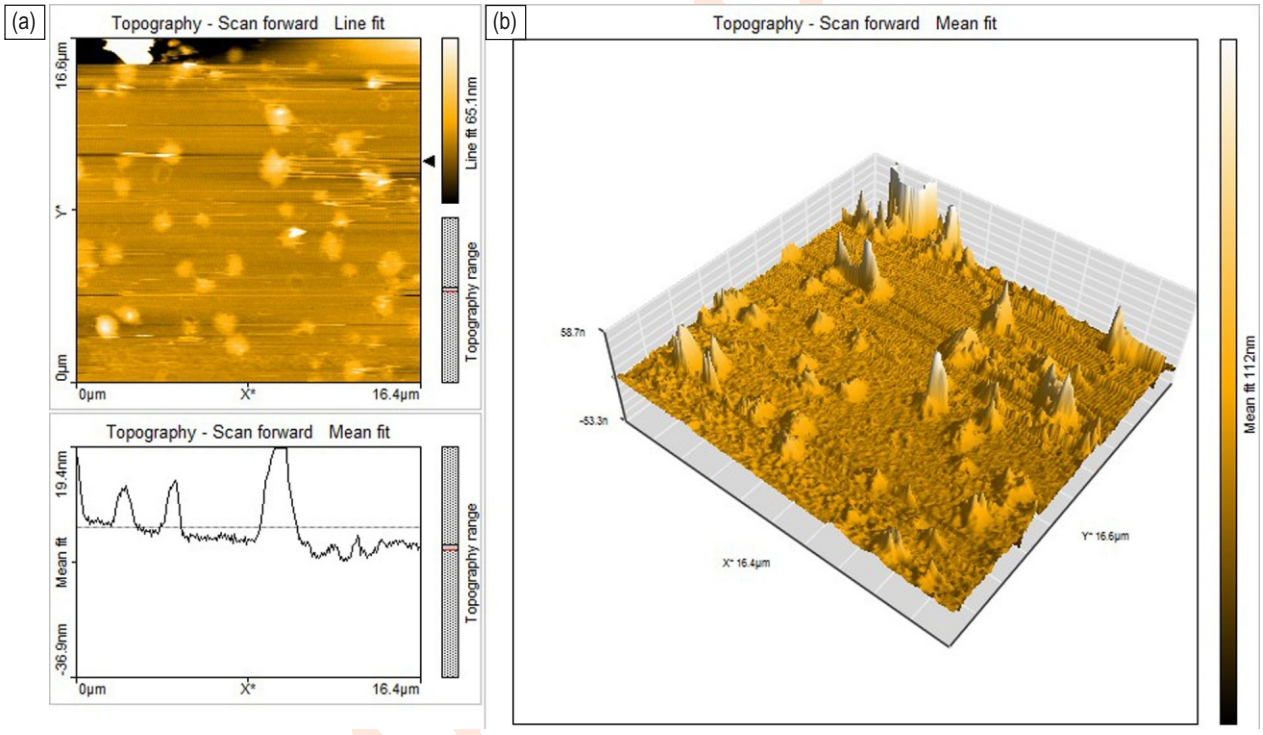

Fig. 4: Atomic force microscopic images of ZnO nanoparticles.

of the green synthesized ZnO NPs (Fig. 2b). High percentage occurrence of Zn and O is indicative of ZnO formation. The chemical constituents present in the flower concentrate might be responsible for the additional peaks. The clear high intensity X-ray diffraction (XRD) pattern reveals the purity and crystalline nature (Fig. 3) of green synthesized ZnO NPs. The seven strong diffraction peaks at 2θ angels of 31.94°, 34.14°, 36.862°, 47.73° and 56.343° correspond to the plane of (100), (002), (101), (102) and (110) reflections, respectively. The peaks indicate the hexagonal phase of ZnO NPs, which was in significant agreement with the standard values (JCPDS file No.036-1451) (Aminuzzaman *et al.,* 2018). The absence of diffraction peaks showed that the synthesized ZnO NPs are pure without any cross-contamination with other molecules. The topographical

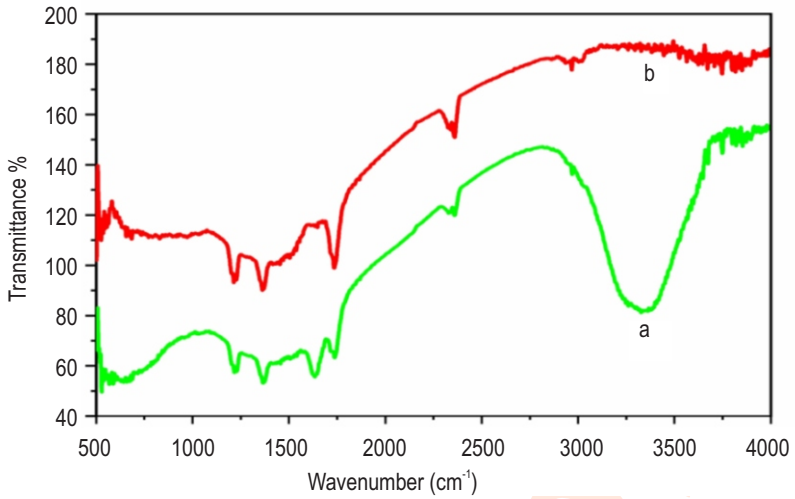

Fig. 5: FT-IR spectrum of *P. tuberosa* flower concentrate (a) and green synthesized ZnO nanoparticles (b).

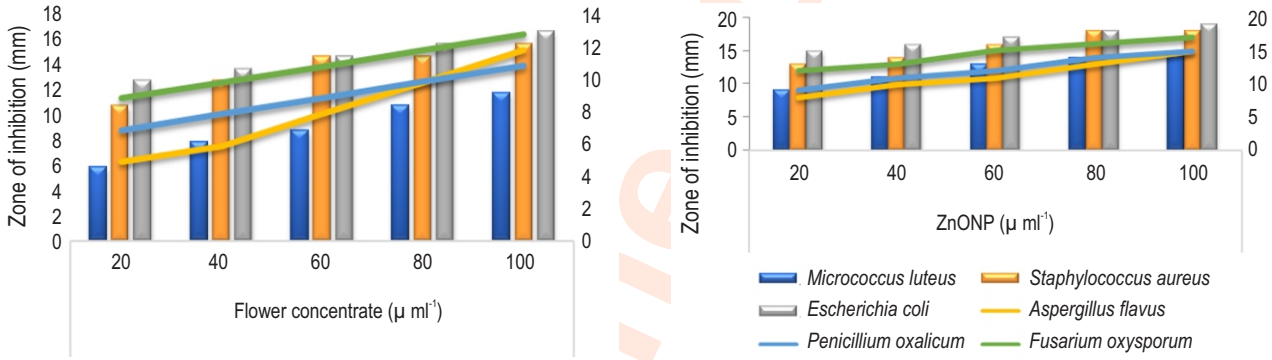

Fig. 6: Inhibitory activities of flower concentrate (a) and ZnO nanoparticles (b) against bacterial and fungal pathogens.

image of green synthesized ZnO NPs was presented in Fig. 4a and b, respectively. The surface nature of biogenic metal nanoparticles was reported to influence the efficiency (Narayanan and Sakthivel, 2011). The atomic force micrograph images confirm the homogeneous, smooth, small grains of NPs, densely packed throughout the surface of scanned area. The size of nanoparticles was found to be 80 nm. The particle size of synthesized ZnO NPs was in close agreement with the previous findings of Rajendran *et al.* (2021).

FT-IR spectra of the flower concentrate and ZnO NPs is presented in Fig. 5a,b, respectively. The peak at 3355 cm^{-1} corresponds to the stretching vibrations of O-H group. It is postulated that during the biosynthesis process, the hydroxyl group (OH) of the flower concentrate is supposed to interact with zinc ions and leads to the formation of ZnO NPs. The broad band illustrates the crystalline nature of the nanoparticles. The peak at 1629 cm^{-1} represent C=C stretching vibrations of aromatic rings. Short peaks at 1370 cm^{-1} and 1216 cm^{-1} are associated with O-H and C-N stretching vibrations. Absorption at 1200 to 1350 cm^{-1} and 1000 to1250 cm^{-1} represents C-N stretching peak of aromatic amines and aliphatic amines. The region between 400 and 600 cm^{-1} represents the presence of metal-oxygen complex (Khan *et al.,* 2023). A shift in the peaks was observed in FT-IR spectum after the bioreduction of ZnO-NPs at 3352-3429 cm^{-1}, 2391-2931 cm^{-1}, 1647-1637 cm^{-1}, 1370-1356 cm^{-1}, 1216-1214 cm^{-1} and 526-503 cm^{-1}, respectively. It is evident from the FT-IR spectrum that the phytochemical constituents present in the flower concentrate reduce and stabilize zinc ions, which is in agreement with the previous reports Li *et al.* (2020). The spectral results were consistent with the reports of Senthilkumar *et al.* (2017).

The antimicrobial activity of the flower concentrate and ZnO NPs was assessed using agar well diffusion method (Fig. 6). Susceptibility of bacteria to ZnO NPs was found to be greater than that of fungi. It is evident from the results that out of the three

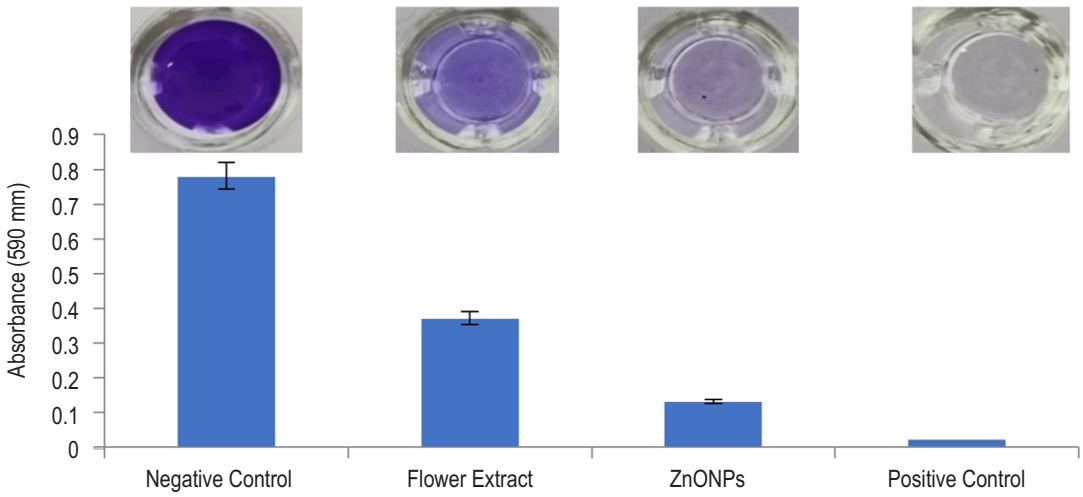

Fig. 7: Inhibitory efficiency of biosynthesized ZnO nanoparticles and flower concentrate on biofilm formation in *P. aeruginosa*.

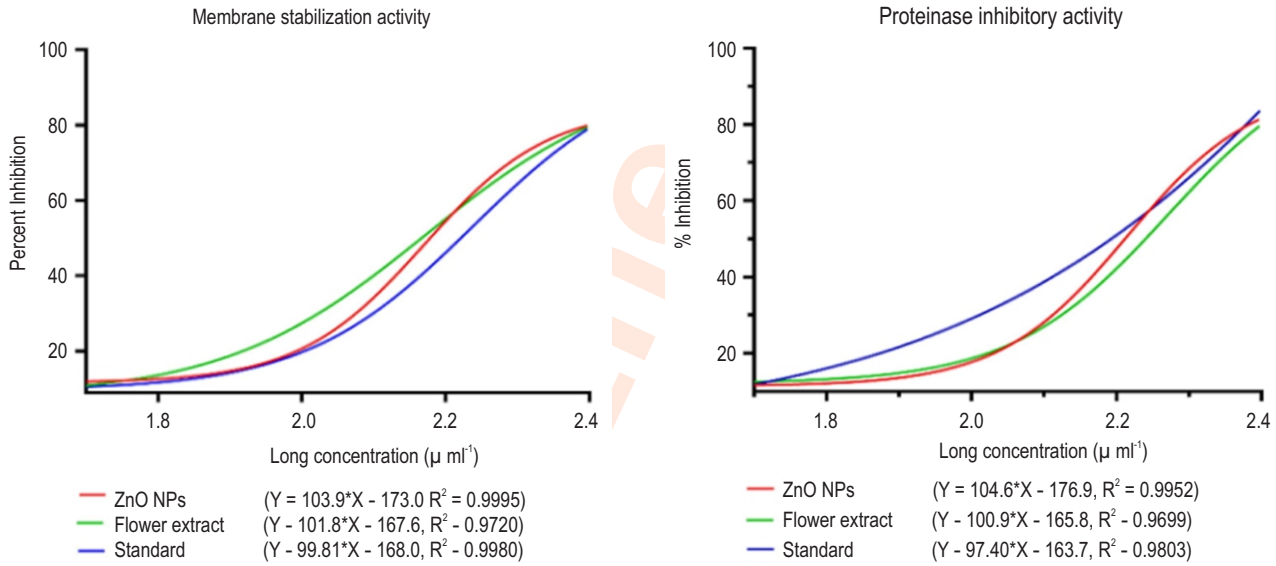

Fig. 8: Dose response curve for anti- inflammatory activity of ZnO nanoparticles, flower concentrate of *P. tuberosa* and standard drug (Aceclofenac).

bacterial pathogens, *M. luteus* was found to be highly resistant with a minimum inhibition zone of 15 mm at 100 µl ml^{-1} of ZnO NPs, followed by *S. aureus* (18 mm) and *E. coli* (19 mm). Concentration dependent inhibitory potential of flower concentrate and ZnO Nps against microbial pathogens was observed. Earlier studies have illustrated the bactericidal activity of ZnO NPs, however, the underlying mechanism was least explored (Yusof *et al.,* 2021). Nagarajan and Kumaraguru (2013) reported that the ZnO NPs interact with the membrane proteins and lipid bilayer and alter the cell permeability of the bacteria. Bactericidal and fungicidal activity of green synthesized ZnO NPs implies its applicability in the sunscreen protectors and in antiseptic ointments. Similar to the results obtained in this study, a high degree of antibacterial efficiency of green synthesized ZnO NPs using plantain peel extract was observed by Imade *et al.* (2022).

Biofilms are polymeric substances produced by certain but not all bacteria. Yusof *et al.* (2021) reported that pathogenic bacteria evade antibiotic susceptibility by biofilm formation. Fig. 7 illustrates the biofilm inhibitory efficiency of *P. tuberosa* flower concentrate and ZnO NPs. Bio-film inhibitory efficiency was found to be greater with ZnO NPs than the flower concentrate. Dose-

dependent decrease in biofilm formation by *P. aeruginosa* was observed in this study. The findings reveal the potential of *P. tuberosa* flower concentrate and ZnO NPs in the treatment of skin infections. Release of Zn^{2+} from ZnO NPs was reported to suppress the peptidoglycan synthesis in pathogenic bacteria by inhibiting the enzymatic action of DapE protein (Khan *et al.,* 2014). The biofilm inhibitory efficiency of ZnO NPs observed in this study substantiates the findings of Abdelghafar *et al.* (2022).

Proteinase inhibitory and HRBC membrane stabilization efficiency of flower concentrate and ZnO NPs is presented in Fig. 8. Both the flower concentrate and ZnO NPs effectively inhibited the heat induced haemolysis. *In-vitro* anti-inflammatory studies revealed that the membrane stabilization efficiency of ZnO NPs (80.7%) was at par with that of reference standard Aspirin (78.7%). In addition, the proteinase inhibitory activity of flower concentrate and ZnO NPs was found to be 78.3% and 80.4%, respectively. The results illustrate that the flower concentrate and ZnO NPs minimize the tissue damage and progression of inflammation by membrane stabilization. Yesmin *et al.* (2020) reported the anti-inflammatory efficiency of root extract of *P. chaba* by precluding the discharge of lytic enzymes and other active inflammatory mediators.

Similar to the results obtained in this study, Zahoor *et al.* (2023) reported that the anti-inflammatory activity of biosynthesized ZnO NPs using the leaves of *Senecio chrysanthemoides* was at par with that of the standard drug diclofenac and it was found to be greater than that of the leaf extract. Good optical, piezoelectric, and semiconducting properties together with biodegradable, biocompatible and non-toxic nature of ZnO nanoparticles make them as an excellent choice for use in medical applications (Aderibigbe, 2024). Furthermore, Saemi *et al.* (2021) reported that zinc oxide nanoparticles penetrate the nuclear membrane and cause irreversible DNA damage, inducing cell death in microbes. It is evident from FT-IR analysis that the green synthesized ZnO nanoparticles has a -OH group that permits it to dissolve at a slow rate in acidic as well as in strong basic environments. The above character makes the green synthesized ZnO NPs as an excellent choice for use as pharmaceutical excipient in skin ointments and cosmetics.

This investigation provides a simple, cost-effective, eco-friendly green approach in the synthesis of zinc oxide nanoparticles (ZnO Nps). The novelty of this study is that the results provide an insight in the possible application of *P. tuberosa* flowers and green synthesized ZnO NPs as a potential anti-biofilm agent with antimicrobial and anti-inflammatory efficiency. Reactive oxygen species (ROS) formation might be one of the reasons for antimicrobial potential. Antifungal efficacy of ZnO NPs reported in this study is more convincing and one of the few reports available till date. The results pay way for the possible utilization of *P. tuberosa* flowers and green synthesized ZnO NPs to overcome skin infections induced by biofilm forming pathogens. Thereby the green synthesis of ZnO NPs using the flowers of *P. tuberosa* put forward their potential application in medicinal nanoscience to mitigate myriad health maladies. Green synthesis of ZnO NPs prevents the release of harmful by-products and undesirable interaction with other biological systems in the host organism. Therefore, *P. tuberosa* flower concentrate and ZnO NPs can be efficiently utilized as a component in lotions, ointments and creams for dermatological applications due to its antimicrobial quality. Further course of study is in progress to carry out the analysis with the flowers collected from different species of the genus *Polianthes.*

Acknowledgements

The authors thank Thiagarajar College Management for providing the infrastructure facilities. BR and J thank the Tamil Nadu Directorate of Collegiate Education (TN-DCE) for providing the research fellowship.

Authors' contribution: R.M. Murugappan: Designed the study, carried out the statistical analysis, interpretation of data and drafted the manuscript; **S. B. Begum:** Technical assistance; **J.J. A. Christy:** Carried out the anti-microbial activity, interpretation of data and figures; **B.R. Harisma and M. Revathy:** Performed bio-film inhibition assay and anti-inflammatory activity.

Funding: Partial financial support was received from Tamil Nadu Directorate of Collegiate Education (TN-DCE).

Research content: The research content of manuscript is original and has not been published elsewhere.

Ethical approval: Not Applicable.

Conflict of interest: The authors declare that they have no conflict of interest.

Data availability: All the data analysed for this study are included. Any extra data of interest if needed are available from the corresponding author upon reasonable request.

Consent to publish: All authors agree to publish the paper in *Journal of Environmental Biology.*

References

Abdelghafar, A., N. Yousef and M. Askoura: Zinc oxide nanoparticles reduce biofilm formation, synergize antibiotics action and attenuate *Staphylococcus aureus* virulence in host; an important message to clinicians. *BMC Microbiology,* **22**, 244 (2022).

Aderibigbe, B.A.: Zinc oxide nanoparticles in biomedical applications: Advances in synthesis, antimicrobial properties, and toxicity considerations. *Nanotechnol. Modern Antimicr. Antiv. Applic.,* pp. 119–149 (2024).

Agidew, M.G.: Phytochemical analysis of some selected traditional medicinal plants in Ethiopia. *Bull. Natl. Res. Cen.,* **46**, 87 (2022).

Alghuthaymi, M.A., S. Patil, R. Chandrasekaran, M. Krishnan, U. Krishnan and K.A. Abd-Elsalam: *Polianthes tuberosa*-mediated silver nanoparticles from flower extract and assessment of their antibacterial and anticancer potential: An In Vitro Approach. *Plants,* **12**, 1261–1261 (2023).

Alhujaily, M., S. Albukhaty, M. Yusuf, M.K.A. Mohammed, G.M. Sulaiman, H. Al-Karagoly, A.A. Alyamani, J. Albaqami and F.A. AlMalki: Recent advances in plant-mediated zinc oxide nanoparticles with their significant biomedical properties. *Bioengineering,* **9**, 541 (2022).

Alves, A., E. Sousa, A. Kijjoa and M. Pinto: Marine-derived compounds with potential use as cosmeceuticals and nutricosmetics. *Molecules,* **25**, 2536 (2020).

Aminuzzaman, M., L.P. Ying, W.S. Goh and A. Watanabe: Green synthesis of zinc oxide nanoparticles using aqueous extract of *Garcinia mangostana* fruit pericarp and their photocatalytic activity. *Bull. Mater. Sci.,* **41**, 50 (2018).

Anantha, T.S., S. Natarajan and H.R. Cama: Physiochemical and biological properties of glycoproteins isolated from the plasma of different species of animals. *Biochem. J*., **96**, 281-288 (1956).

Chaudhuri, S.K and L. Malodia: Biosynthesis of zinc oxide nanoparticles using leaf extract of *Calotropis gigantea*: characterization and its evaluation on tree seedling growth in nursery stage. *Appl. Nanosci.*, **7**, 501–512 (2017).

El-Belely, E.F., M.M.S. Farag, H.A. Said, A.S. Amin, E. Azab, A.A. Gobouri and A. Fouda: Green synthesis of zinc oxide nanoparticles (ZnO-NPs) using *Arthrospira platensis* (Class: Cyanophyceae) and evaluation of their biomedical activities. *Nanomaterials,* **11**, 95 (2021).

Fulindi, R.B., J.D. Rodrigues, T.W.L. Barbosa, A.D.G. Garcia, F. de A. La Porta, S. Pratavieira, L.A. Chiavacci, J.P.A. Junior, P.I. Da Coata and L.R. Martinez: Zinc-based nanoparticles reduce bacterial biofilm formation. *Microbiol. Spectrum.,* **11**, e04831-22 (2023).

Gao, F., Y. Wu and M. Wang: Identification and antifungal activity of an actinomycete strain against *Alternaria* spp. S*pan. J. Agricul. Res.*, **12**, 1158 (2014).

Harborne, J.B: Phytochemcial Methods. Chapman and Hall Ltd., London, pp. 49-188 (1973).

Imade, E.E., T.O. Ajiboye, A.E. Fadiji, D.C. Onwudiwe and O.O. Babalola: Green synthesis of zinc oxide nanoparticles using plantain peel extracts and the evaluation of their antibacterial activity. *Sci. Afric.,* **16**, e01152 (2022).

Khan, A.U.H., Y. Liu, C. Fang, R. Naidu, H.K. Shon, Z. Rogers and R. Dharmarajan: A comprehensive physicochemical characterization of zinc oxide nanoparticles extracted from sunscreens and wastewaters. *Environ. Adv.,* **12**, 100381 (2023).

Khan, S.T., M. Ahamed, J. Musarrat and A.A. Al-Khedhairy: Anti-biofilm and antibacterial activities of zinc oxide nanoparticles against the oral opportunistic pathogens *Rothia dentocariosa* and *Rothia mucilaginosa. Eur. J. Oral. Sci.,* **122**, 397–403 (2014).

Krol, A., P. Pomastowski, K. Rafinska, V. Railean-Plugaru and B. Buszewski: Zinc oxide nanoparticles: Synthesis, antiseptic activity and toxicity mechanism. *Adv. Coll. Interf. Sci.,* **249**, 37–52 (2017).

Kumar, B., R., A. Fikadu, A. Bachheti and A. Husen: Biogenic fabrication of nanomaterials from flower-based chemical compounds, characterization and their various applications: A review. *Saudi J. Biol. Sci.*, **27**, 2551–2562 (2020).

Kutty, N.N. and A. Mitra: Profiling of volatile and non-volatile metabolites in *Polianthes tuberosa* L. flowers reveals intraspecific variation among cultivars. *Phytochemistry,* **162**, 10–20 (2019).

Li, Y., C. Liao and S.C. Tjong: Recent advances in zinc oxide nanostructures with antimicrobial activities. *Int. J. Mol. Sci.,* **21**, 8836 (2020).

Manjamalai, A., R. Sardar, S. Singh, C. Guruvayoorappan and V.M.B. Grace: Analysis of phytochemical constituents and antimicrobial activity of some medicinal plants in Tamil Nadu, India. *Global J. Biotechnol. Biochem.,* **5**, 120-128 (2010).

McIntosh, K., A. Smith, L.k. Young, M. Leitch, A. Tiwari, C. Reddy, G. O'Neil, M. Liberatore, M. Chandler and G. Baki: Alkenones as a promising green alternative for waxes in cosmetics and personal care products. *Cosmetics,* **5**, 34 (2018).

Nagarajan, S. and K.A. Kumaraguru: Extracellular synthesis of zinc oxide nanoparticle using seaweeds of gulf of Mannar, India. *J. Nanobiotechnology,* **11**, 39 (2013).

Naseer, M., U. Aslam, B. Khalid and B. Chen: Green route to synthesize zinc oxide nanoparticles using leaf extracts of *Cassia fistula* and *Melia azadarach* and their antibacterial potential. *Sci. Rep.,* **10**, 9055 (2020).

Nazir, A., M. Raza, M. Abbas, S. Abbas, A. Ali, Z. Ali, U. Younas, S.H. Al-Mijalli and M. Iqbal: Microwave assisted green synthesis of ZnO nanoparticles using *Rumex dentatus* leaf extract: photocatalytic and antibacterial potential evaluation. *Zeitschrift Für Physikalische Chemie.,* **236**, 1203–1217 (2022).

Nithya Deva Krupa, A. and V. Raghavan: Biosynthesis of silver nanoparticles using *Aegle marmelos* (Bael) fruit extract and its application to prevent adhesion of bacteria: A strategy to control microfouling. *Bioinorg. Chem. Appl.,* **2014**, 1–8 (2014).

O'Toole, G.A., L.A. Pratt, P.I. Watnick, D.K. Newman, V.B. Weaver and R. Kolter: Genetic approaches to study of biofilms. *Biofilms,* **310**, 91–109 (1999).

Patravale, V.B., A.A. Date and R.M. Kulkarni: Nanosuspensions: a promising drug delivery strategy. *J. Pharm. Pharmacol.,* **56**, 827–840 (2004).

Qureshi, A., Y.C. Gupta, A. Abrol and P. Sharma: Prosptest of value addition in jasmine and tuberose. *J. Emerg. Technol. Innov. Res.,* **5**, 263–277 (2018).

Raha, S. and M. Ahmaruzzaman: ZnO nanostructured materials and their potential applications: Progress, challenges and perspectives. *Nanos. Adv.,* **4**, 1868–1925 (2022).

Rajendran, N.K., B.P, George, N.N. Houreld and H. Abrahamse: Synthesis of zinc oxide nanoparticles using *Rubus fairholmianus* root extract and their activity against pathogenic bacteria. *Molecules,* **26**, 3029 (2021).

Sadique, J., W.A. Al-Rqobahs, M.F. Bughaith and A.R. El-Gindy: The bio-activity of certain medicinal plants on the stabilization of RBC membrane system. *Fitoterapia,* **60**, 525–532 (1989).

Saemi, R., E. Taghavi, H. Jafarizadeh-Malmiri and N. Anarjan: Fabrication of green ZnO nanoparticles using walnut leaf extract to develop an antibacterial film based on polyethylene–starch–ZnO NPs. *Green Process. Synth.,* **10**, 112–124 (2021).

Salam, H.A., R. Sivaraj and R. Venckatesh: Green synthesis and characterization of zinc oxide nanoparticles from *Ocimum basilicum* L. var. purpurascens Benth.-Lamiaceae leaf extract. *Mater. Lett.,* **131**, 16–18 (2014).

Sangeetha, G., S. Rajeshwari and R. Venckatesh: Green synthesis of zinc oxide nanoparticles by *Aloe barbadensis* miller leaf extract: Structure and optical properties. *Mat. Res. Bull.*, **46**, 2560–2566 (2011).

Sepasgozar, S.M.E., S. Mohseni, B. Feizyzadeh and A. Morsali: Green synthesis of zinc oxide and copper oxide nanoparticles using *Achillea nobilis* extract and evaluating their antioxidant and antibacterial properties. *Bull. Mater. Sci.,* **44**, 129 (2021).

Setiani, N.A., D.L. Aulifa, Selynita and E. Septiningsih: Phytochemical screening and antibacterial activity of flower, stem, and tuber of *Polianthes tuberosa* L. against acne-inducing bacteria. *Adv. Hlth. Sci. Res.,* **26**, 92-95 (2020).

Sidhu, A.K., N. Verma and P. Kaushal: Role of biogenic capping agents in the synthesis of metallic nanoparticles and evaluation of their therapeutic potential. *Front. Nanotechnol.,* **3,** 801620 (2022).

Smania, A., F.D. Monache, E.F.A. Smânia and R.S. Cuneo: Antibacterial activity of steroidal compounds isolated from *Ganoderma applanatum* (Pers.) Pat. (Aphyllophoromycetideae) fruit body. *Int. J. Med. Mushroom.*, **1**, 325330 (1999).

Sofowara, A.: Medicinal Plants and Traditional Medicine in Africa. Spectrum Books Ltd, Ibadan, Nigeria, 289 pages (1993).

Suryakoppa, K.S., R. Appadurai, K. Byrappa and M.H.M. Khan: Phytochemical analysis of UV active and inactive bioactive compounds present in *Polianthes tuberosa* (Linn.) flower. *J. Sep. Sci.,* **44**, 3376–3385 (2021).

Vestby, L.K., T. Gronseth, R. Simm and L.L. Nesse: Bacterial biofilm and its role in the pathogenesis of disease. *Antibiotics*, **9**, 59 (2020).

Wang, H., L. Lin, L. Tan, H.Y. Yu, J.W. Cheng and Y. Pan: Molecular pathways underlying inhibitory effect of antimicrobial peptide Nal-P-113 on bacteria biofilms formation of *Porphyromonas gingivalis* W83 by DNA microarray. *BMC Microbiol.,* **17**, 37 (2017).

Yang, B., F. Qi, J. Tan, T. Yu and C. Qu: Study of green synthesis of ultrasmall gold nanoparticles using citrus sinensis peel. *Appl. Sci.,* **9**, 2423 (2019).

Yesmin, S., A. Paul, T. Naz, A.B.M.A. Rahman, S.F. Akhter, M.I.I. Wahed, T.B. Emran and S.A. Siddiqui: Membrane stabilization as a mechanism of the anti-inflammatory activity of ethanolic root extract of Choi (*Piper chaba*). *Clin. Phytosci.,* **6**, 1-10 (2020).

Yusof, H.M., N.A. Rahman, R. Mohamad, U.H. Zaidan and A.A. Samsudin: Antibacterial potential of biosynthesized zinc oxide nanoparticles against poultry-associated foodborne pathogens: an *in vitro* study. *Animals,* **11**, 2093 (2021).

Zahoor, S., S. Sheraz, D.F. Shams, G. Rehman, S. Nayab, M.I.A. Shah, M. Ateeq, S.K. Shah, T. Ahmad, S. Shams and W. Khan: Biosynthesis and anti-inflammatory activity of zinc oxide nanoparticles using leaf extract of *Senecio chrysanthemoides*. *BioMed Res. Int.,* **2023**, e3280708 (2023).